

NATIONAL ADVISORY COMMITTEE FOR AERONAUTICS

TECHNICAL NOTE 3360

SOME EFFECTS OF PROPELLER OPERATION AND LOCATION
ON ABILITY OF A WING WITH PLAIN FLAPS TO DEFLECT PROPELLER
SLIPSTREAMS DOWNWARD FOR VERTICAL TAKE-OFF

By John W. Draper and Richard E. Kuhn

Langley Aeronautical Laboratory
Langley Field, Va.



Washington

January 1955

AFM C
TECHNICAL NOTE
AFM 221



TECHNICAL NOTE 3360

SOME EFFECTS OF PROPELLER OPERATION AND LOCATION
ON ABILITY OF A WING WITH PLAIN FLAPS TO DEFLECT PROPELLER
SLIPSTREAMS DOWNWARD FOR VERTICAL TAKE-OFF

By John W. Draper and Richard E. Kuhn

SUMMARY

An investigation has been conducted to determine the effects of several factors associated with the propeller installation on the ability of a wing with plain flaps to deflect a propeller slipstream downward as a means for achieving vertical take-off. The factors considered were propeller blade angle, mode of propeller rotation, propeller location, and ratio of wing chord to propeller diameter. The investigation was made at zero forward speed on models of semispan wings.

Lowering the thrust axis appreciably below the wing-chord plane reduced the diving moment of the flaps but had little effect on the turning angle of the slipstream or on the ratio of resultant force to thrust when the thrust axis was lowered only 20 percent of the propeller radius. The best turning effectiveness was obtained when the propeller mode of rotation was such that the outboard propeller rotated against the tip vortex and the inboard propeller rotated in the opposite direction. On the basis of tests with flat plates of various chords, the best turning angle was obtained with a ratio of wing chord to propeller diameter equal to 1.00, which was the largest ratio investigated; however, increasing the ratio of wing chord to propeller diameter from 0.75 to 1.00 led to only a small improvement in turning effectiveness but caused a large increase in the diving moment.

INTRODUCTION

An investigation of the effectiveness of monoplane wings and flaps in deflecting propeller slipstreams downward is being conducted at the Langley Aeronautical Laboratory. A part of this investigation is reported in references 1 and 2. The results of reference 1 indicate that a monoplane wing equipped with plain flaps and auxiliary vanes can deflect the slipstream through the large angles approaching the angles required for vertical take-off.

Results are presented herein of a limited investigation of the effects of several variables related to the propeller installation on the turning effectiveness of the wing with plain flaps at zero forward speed. The variables investigated and reported in this paper are as follows: the propeller blade angle, the mode of propeller rotation, the vertical position of the thrust axis, the longitudinal position of the propeller disk, and the ratio of wing chord to propeller diameter.

SYMBOLS

The data presented in this paper are based on the coefficients given below and are presented with reference to the convention of forces, moments, and angles shown in figure 1. It should be noted that the coefficients which are identified by the double prime are based on the dynamic pressure in the propeller slipstream as discussed in references 1 and 2. In this manner, the infinite value of the coefficients at zero forward speed is eliminated.

C_L'' lift coefficient, $\frac{L}{q''S/2}$

C_m'' pitching-moment coefficient, $\frac{M}{q''\bar{c}S/2}$

C_X'' longitudinal-force coefficient, $\frac{X}{q''S/2}$

T_c thrust coefficient, $\frac{T}{q''\pi D^2/4}$

c local wing chord, ft or in.

\bar{c} mean aerodynamic chord of wing, ft or in.

D propeller diameter, ft or in.

L lift, lb

M pitching moment, ft-lb

q free-stream dynamic pressure (zero for these tests), lb/sq ft

q''	dynamic pressure in slipstream (ref. 1), $q + \frac{T}{\pi D^2/4}$, lb/sq ft
R	radius to propeller tip, ft
S	twice area of semispan wing, sq ft
T	thrust per propeller, lb
X	longitudinal force, lb
x	longitudinal position of propeller disk measured from $\bar{c}/4$, ft
z	vertical position of thrust axis measured from mean chord line of wing, ft
$\beta_{.75R}$	propeller blade angle at $0.75R$, deg
δ_f	flap deflection (subscript "30" or "60" indicates percent chord deflected), deg
η''	static-thrust efficiency (ref. 2)
θ	angle between thrust axis and resultant force, deg

APPARATUS AND METHODS

The investigation was conducted on the static-thrust facility (fig. 2) of the Langley 7- by 10-Foot Tunnels Branch. Details of this installation are described in reference 1. The model used for most of the tests is the same as that of reference 1. The geometric characteristics of this model are presented in the following table:

Wing:

Area (semispan), sq ft	5.125
Span (semispan), ft	3.416
Mean aerodynamic chord, ft	1.514
Root chord, ft	1.75
Tip chord, ft	1.25
Airfoil section	NACA 0015
Aspect ratio (full span)	4.55
Taper ratio	0.714

Propellers:

Diameter, ft	2.0
Disk area, sq ft	3.14
Nacelle diameter, ft	0.33
Airfoil section	Clark Y

The tests to determine the effects of propeller blade angle and the direction of propeller rotation were conducted with two propeller-nacelle assemblies mounted on the wing. A plan and section view of this model is shown in figure 3. For some tests this model was equipped with two auxiliary vanes over the hinge line at the 40-percent-chord station. Details of the auxiliary-vane configuration are described in reference 1. The tests to determine the effects of propeller location and of the ratio of wing chord to propeller diameter were conducted by use of the setup shown in figure 4. For these tests, a single propeller was located at the same spanwise station as the inboard propeller shown in figure 3. Although the propeller was independently mounted for these tests, the direct propeller forces have been included in the data presented.

A survey of the dynamic pressure in the slipstream was also made with the propeller mounted as shown in figure 4. For these tests, the propeller blades were reversed so as to direct the slipstream back along the motor nacelle and the support member. A rake of total-pressure tubes was mounted on the support to measure the dynamic pressure.

The investigation of the effects of the ratio of wing chord to propeller diameter was conducted with a series of untapered wings constructed of 1/2-inch plywood, with rounded leading edges and trailing edges that were beveled for the rearward 1-inch chord. This series of flat-plate wings had a 30-inch semispan and chords of 6, 12, 18, and 24 inches. Each wing was equipped with both 30-percent-chord and 60-percent-chord plain flaps, and the gaps at the hinge line were sealed for all tests. The tests were conducted with the blade-angle setting at 8.0° .

All data presented were obtained at zero forward velocity, a dynamic pressure in the slipstream equal to 8.0 pounds per square foot, and a propeller thrust of 25 pounds. Inasmuch as the tests were conducted under static conditions in a large room, none of the corrections that are normally applicable to wind-tunnel investigations were applied. The pitching moments presented are referred to the quarter chord of the mean aerodynamic chord of the wing. Lift, longitudinal force, and pitching moment were measured on a balance at the root of the model. The shaft thrust of each propeller was measured by strain gages on the beams supporting the electric motors inside the nacelles.

RESULTS AND DISCUSSION

The basic data obtained with propeller blade angles of 3.7° and 8° at 0.75 radius for a series of flap settings are presented in figures 5 and 6. The two propeller blade angles corresponded to the condition of maximum static-thrust efficiency ($\beta_{.75R} = 8^\circ$) and to the condition of high ratio of thrust to torque ($\beta_{.75R} = 3.7^\circ$). The static-thrust efficiency was determined by the method of reference 2, which indicated the efficiency of the isolated propeller to be 0.63 for $\beta_{.75R} = 3.7^\circ$ and 0.70 for $\beta_{.75R} = 8^\circ$. When the blades were overlapped, the efficiencies were reduced to 0.57 and 0.65 for $\beta_{.75R} = 3.7^\circ$ and 8° , respectively.

Effect of propeller blade angle.— The effects of blade angle are shown in figure 6 where the 60-percent-chord flap was set at several fixed deflections and the deflection of the 30-percent-chord flap was varied. With the 60-percent-chord flap deflected 60° , two auxiliary vanes were added to maintain flow over the airfoil. Figure 6(d) shows that, for the same thrust, higher turning angles and generally higher ratios of resultant force to thrust were obtained with a lower blade angle. The static-thrust efficiency of the propeller, however, was considerably less at the lower blade angle, and in practical application the amount of resultant force that can be obtained from a given power rather than from a given thrust is important. The effects of propeller static-thrust efficiency are included in the data presented in figure 6(e). The values presented represent the ratio of force to thrust that would be obtained if the propeller were 100-percent efficient. Figure 6(e) presents a comparison of the effects of propeller blade angle on the basis of constant power and indicates that the maximum turning angles are obtained with the lower blade angle but the maximum resultant force is obtained with the higher blade angle. It would be desirable, of course, to obtain both maximum turning angle and maximum resultant force.

The dynamic-pressure survey of the propeller slipstream (fig. 7) indicates that the lower blade angle produces higher velocities near the root of the blades. It may be possible that increases in the turning angle can be effected if the propeller could be designed to obtain maximum static-thrust efficiency and also to maintain high velocities near the root of the blades. In addition, extra care should be taken to minimize the possibility of flow separation from the rear part of the nacelles.

Effect of mode of propeller rotation.— A comparison of the results for two modes of propeller rotation with various flap settings (fig. 8) indicates that, when the outboard propeller is rotating against the tip

vortex (right-hand rotation on right wing tip) and the inboard propeller is rotating in the opposite direction, higher lift coefficients are obtained. This mode of rotation (also used in refs. 1 and 2) results in better turning effectiveness than could be obtained with the opposite direction of rotation, as shown in figure 8(d).

Two factors probably contribute to this result: With the outboard propeller rotating in such a manner as to oppose the tip vortex, the tip losses are reduced; therefore, the lift would be expected to increase. Also, with this mode of rotation there is an upflow on the part of the wing between the nacelles which produces an increase in lift that probably is not completely cancelled by the downflow at the wing tip.

Effect of longitudinal and vertical position of the propeller.— This phase of the investigation was made with one propeller mounted in front of the wing with the thrust axis parallel to the chord plane of the wing (fig. 4). Figure 9 shows the effect of both the vertical and the longitudinal location of the propeller relative to the wing. The advantage of lowering the thrust axis (parallel to the chord plane) is indicated in the pitching-moment data of figure 9(a) where the thrust-axis position z/R of about -0.25 is sufficient to balance out the pitching moment produced by the flap deflections of $\delta_{f30} = 30^\circ$

and $\delta_{f60} = 30^\circ$. The turning effectiveness (figs. 9(b) and (c)) was very little affected by the vertical movement of the thrust axis within $\pm 0.20R$. At the larger distances from the chord plane the turning angle was decreased. For values of z/R within ± 0.20 there was little effect of the longitudinal position x/R on the aerodynamic characteristics of the wing for the two positions investigated.

Effect of ratio of wing chord to propeller diameter.— The effect of the ratio of wing chord to propeller diameter was investigated by means of flat-plate wings, as previously described. The results (figs. 10 and 11) are presented primarily to determine trends. A direct comparison of these data in coefficient form with those of the basic model would not be appropriate because of the variations in wing geometry involved; therefore, the forces and moments for these tests are presented in pounds and foot-pounds, respectively. The points representative of the ratios of wing chord to propeller diameter for the airfoil model are also presented in these figures in pounds and foot-pounds. The tests were made at zero forward speed ($T_c = 1.0$) with a slipstream dynamic pressure $q = 8.0$ pounds per square foot. The pitching moments are measured about the quarter chord of the mean aerodynamic chord of the wing.

The basic data are presented in figure 10 and are cross-plotted for two flap settings in figure 11. It appears that the highest turning angle was obtained with the largest ratio of wing chord to propeller diameter ($c/D = 1.0$); however, the improvement was small for an increase

in the ratios of wing chord to propeller diameter from 0.75 to 1.00. This range of c/D ratio shows low ratios of resultant force to thrust and large negative pitching moments.

CONCLUSIONS

An investigation of some effects of propeller operation and location on the ability of a wing with plain sealed flaps to deflect the propeller slipstream through large angles indicate the following conclusions:

1. The best turning effectiveness was obtained when the propeller mode of rotation was such that the outboard propeller rotated against the tip vortex (right-hand rotation on right wing tip) and the inboard propeller rotated in the opposite direction.
2. Lowering the thrust axis below the wing-chord plane appreciably relieved the pitching moments produced by the flaps; moreover, a vertical position of the thrust axis within ± 0.20 of the propeller radius had little effect on the turning effectiveness.
3. On the basis of tests with flat-plate wings of various chords, a chord-diameter ratio of 1.0, which was the largest ratio tested, provided the highest turning angles; however, the improvement was small for chord-diameter ratios between 0.75 and 1.00, and large diving moments were associated with these larger chord-diameter ratios.

Langley Aeronautical Laboratory,
National Advisory Committee for Aeronautics,
Langley Field, Va., October 8, 1954.

REFERENCES

1. Kuhn, Richard E., and Draper, John W.: An Investigation of a Wing-Propeller Configuration Employing Large-Chord Plain Flaps and Large-Diameter Propellers for Low-Speed Flight and Vertical Take-Off. NACA TN 3307, 1954.
2. Draper, John W., and Kuhn, Richard E.: Investigation of the Aerodynamic Characteristics of a Model Wing-Propeller Combination and of the Wing and Propeller Separately at Angles of Attack Up to 90° . NACA TN 3304, 1954.

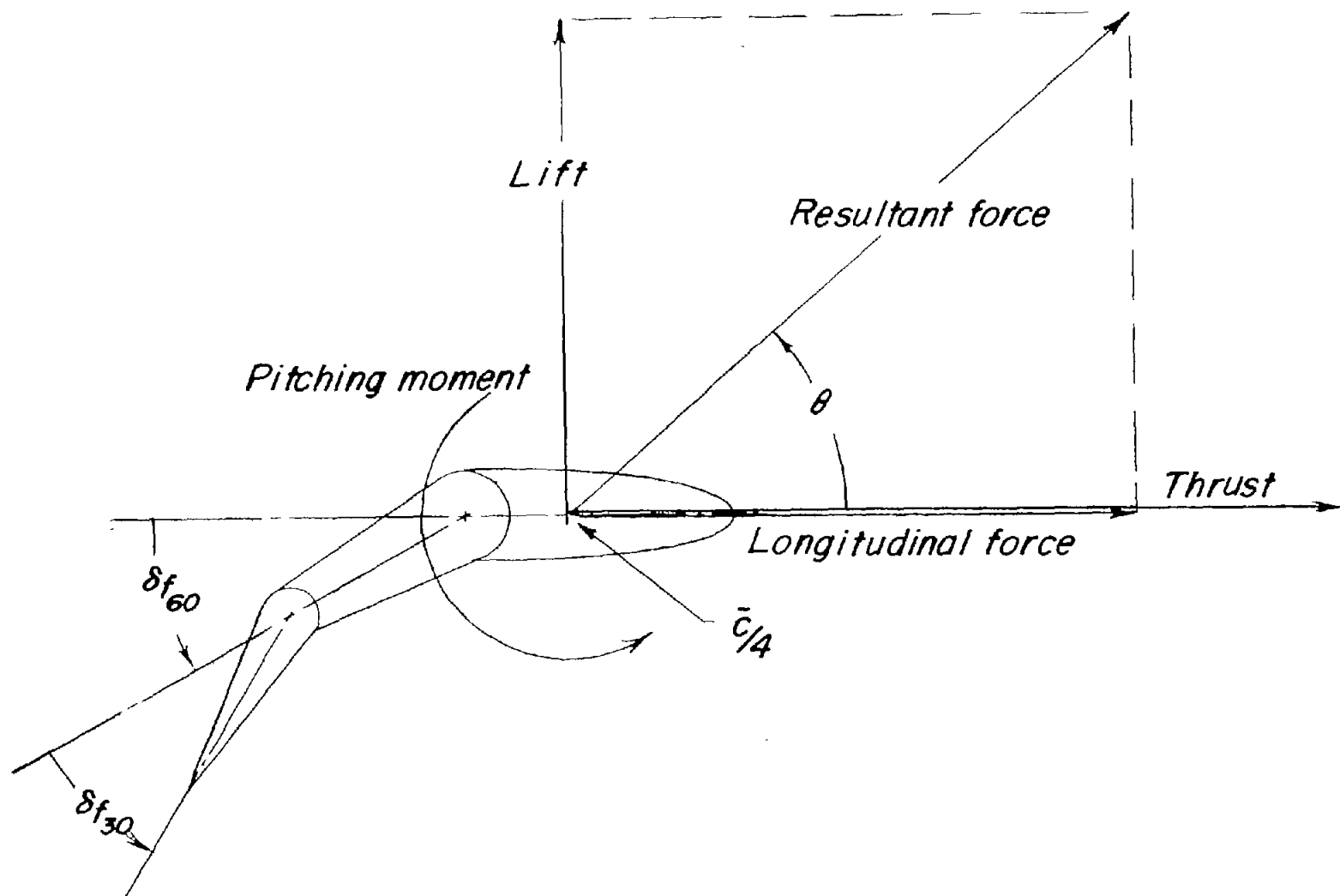


Figure 1.- Sketch of convention used to define positive sense of forces, moments, and angles.

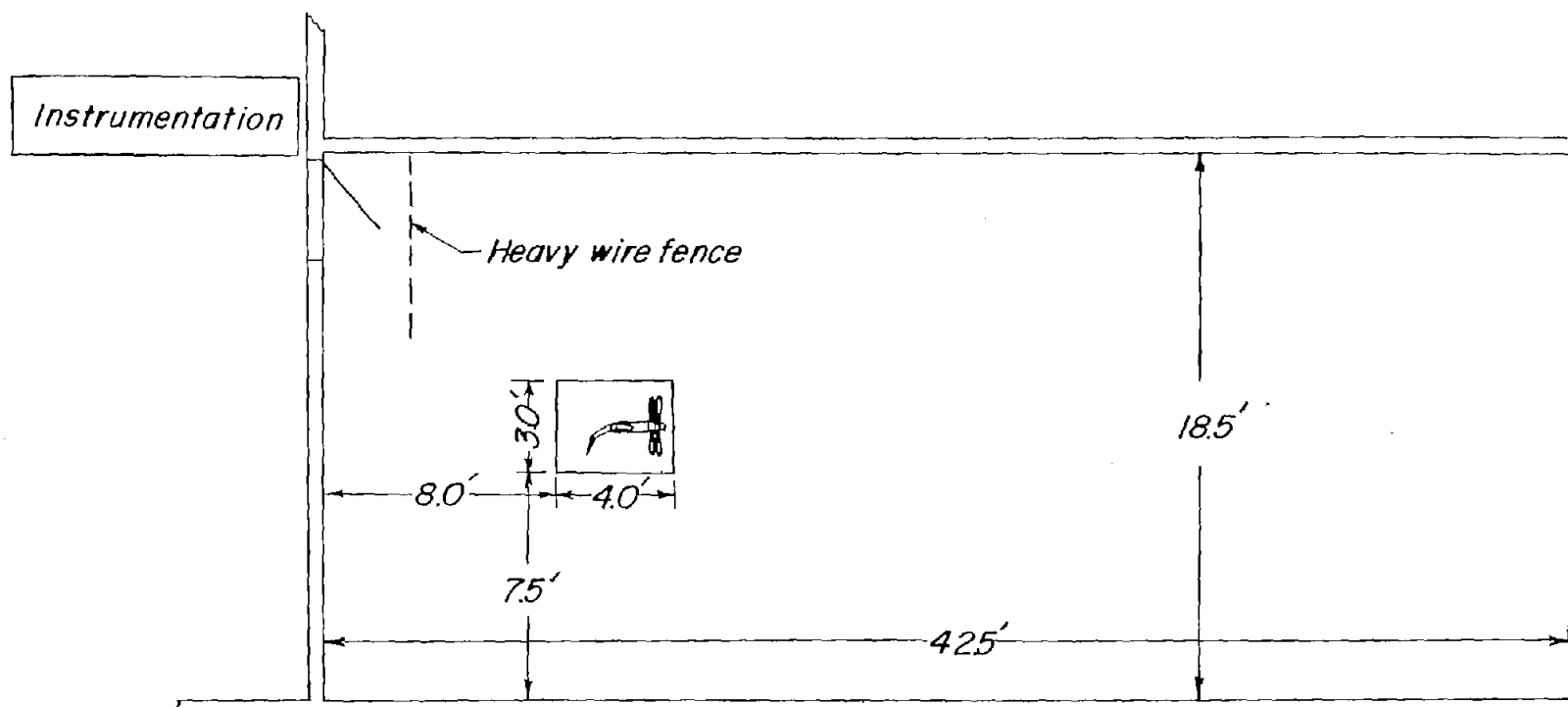


Figure 2.- Plan view of facility used for static-thrust tests.

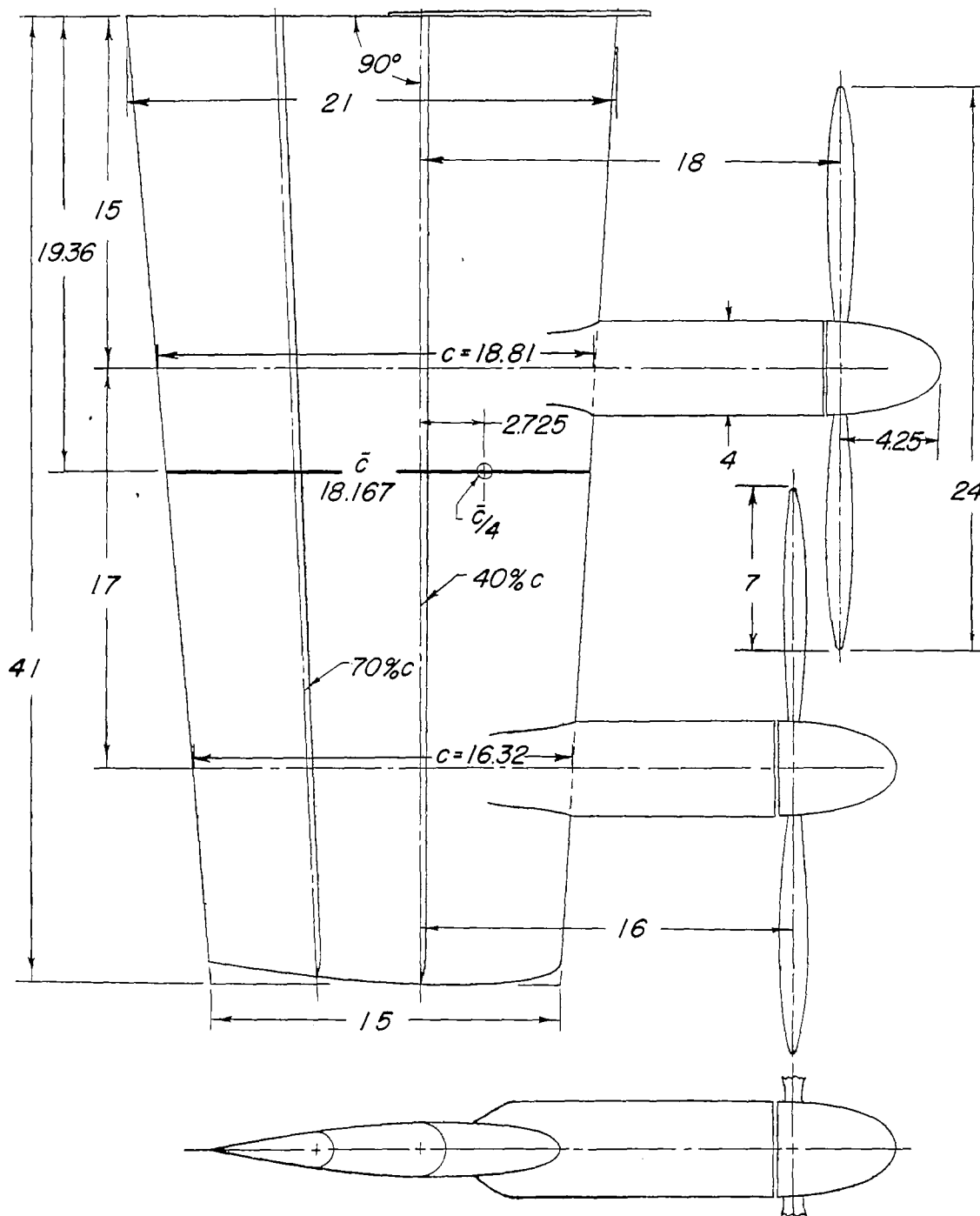
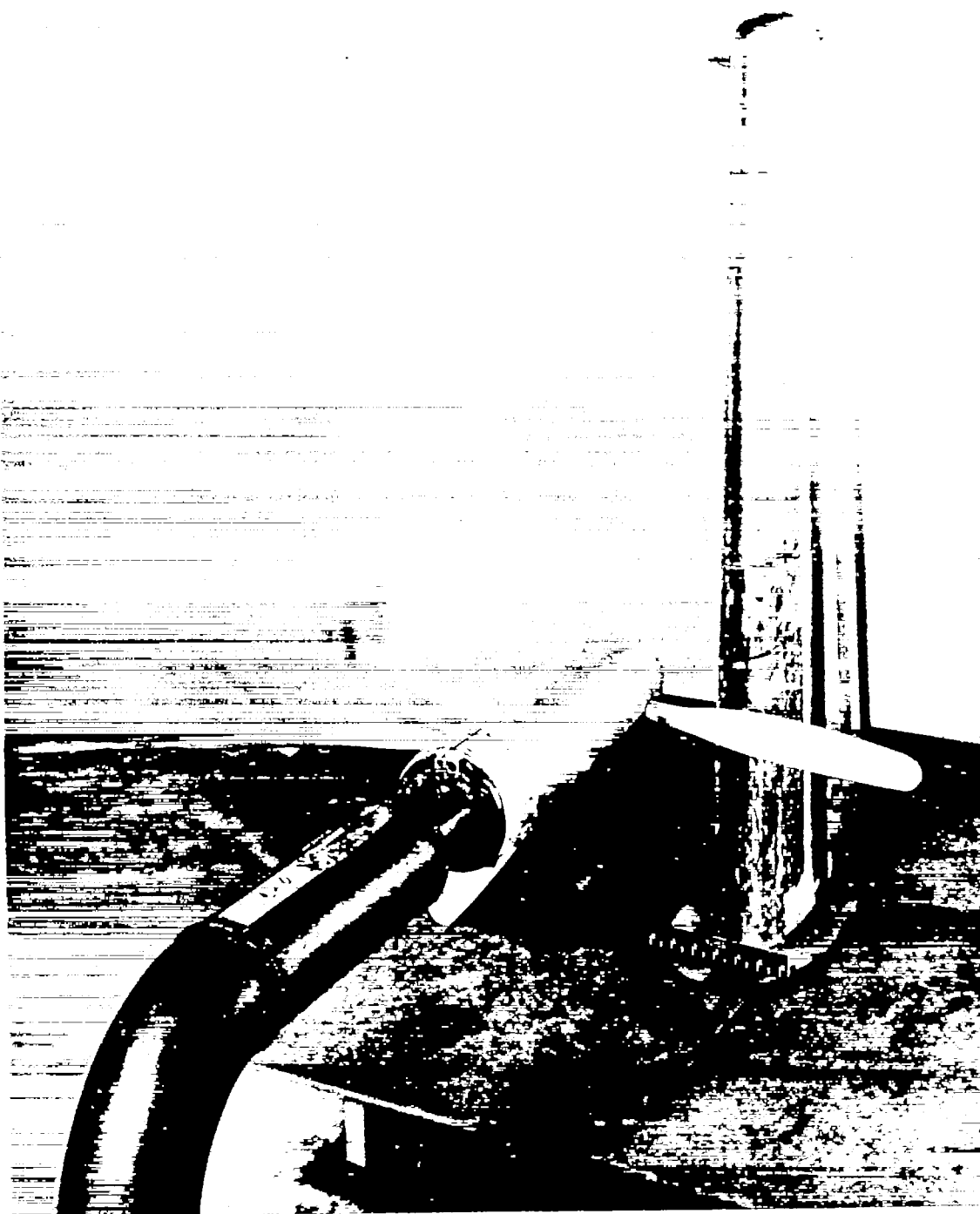
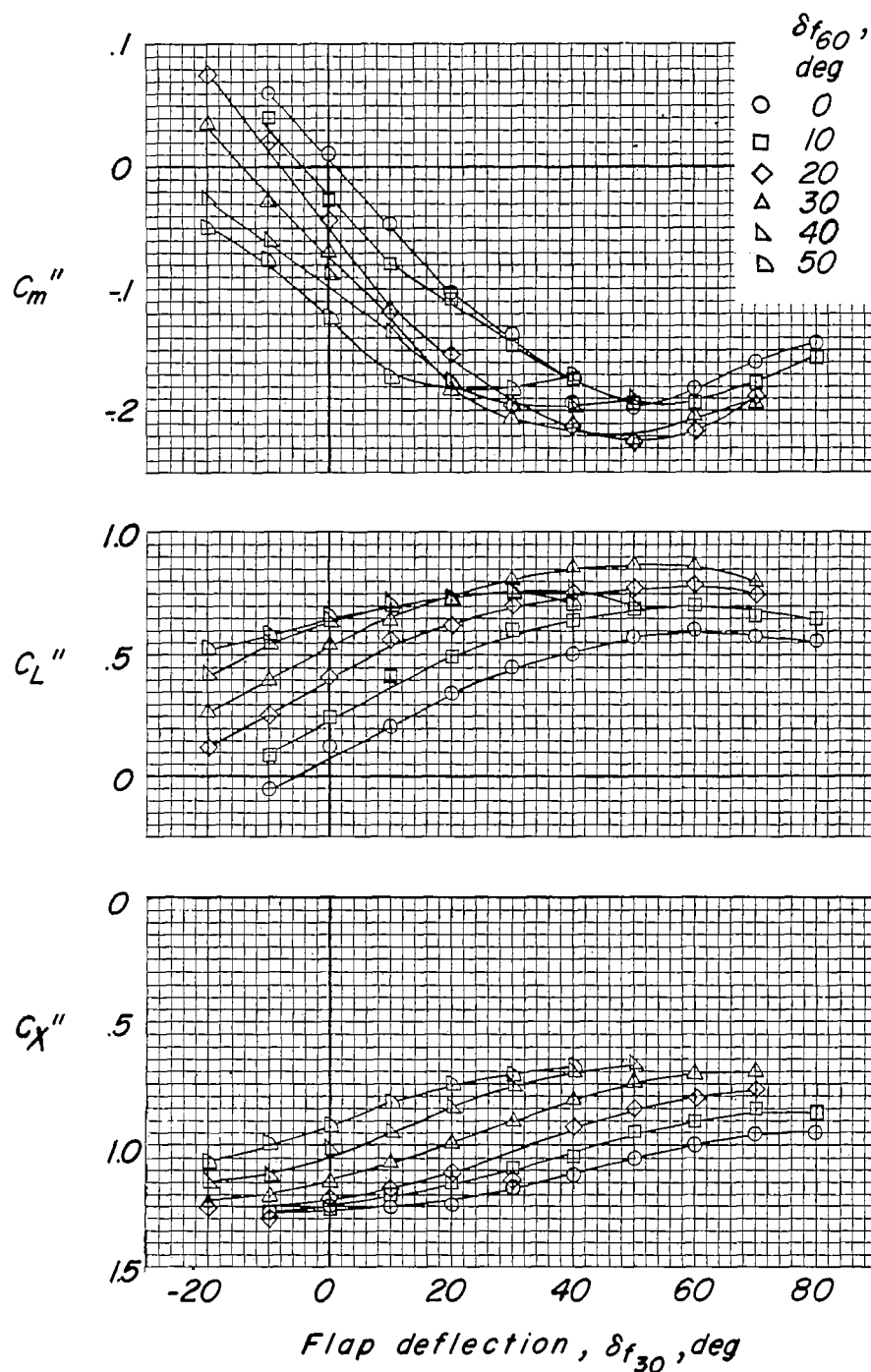


Figure 3.- Plan and cross-sectional views of model. (All dimensions in inches.)



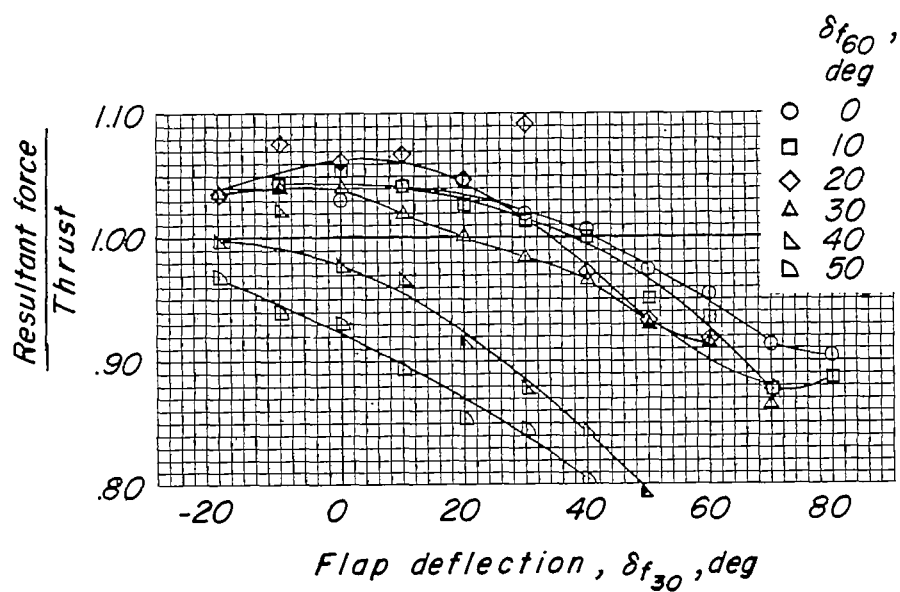
L-85693

Figure 4.- Static-thrust setup used for tests involving changes in propeller position and in ratio of wing chord to propeller diameter.

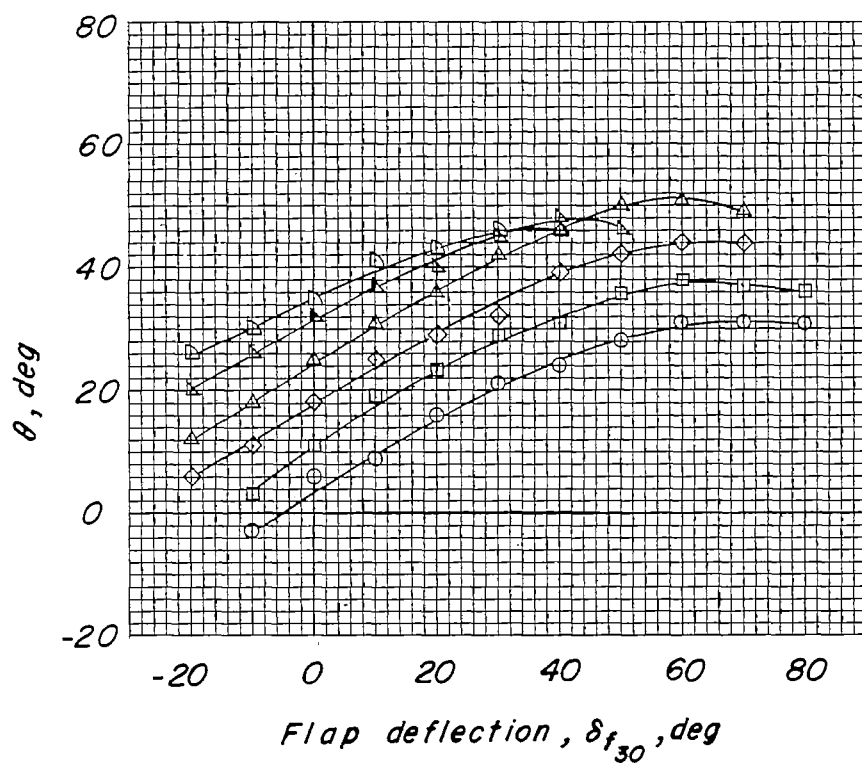


(a) Pitching-moment, lift, and longitudinal-force coefficients.

Figure 5.- Effects of flap deflection on aerodynamic characteristics of wing in propeller slipstream at zero forward velocity. Two propellers; $T_c'' = 1.0$; $\beta_{.75R} = 3.7^\circ$; $q'' = 8.0$ pounds per square foot; NACA 0015 airfoil.

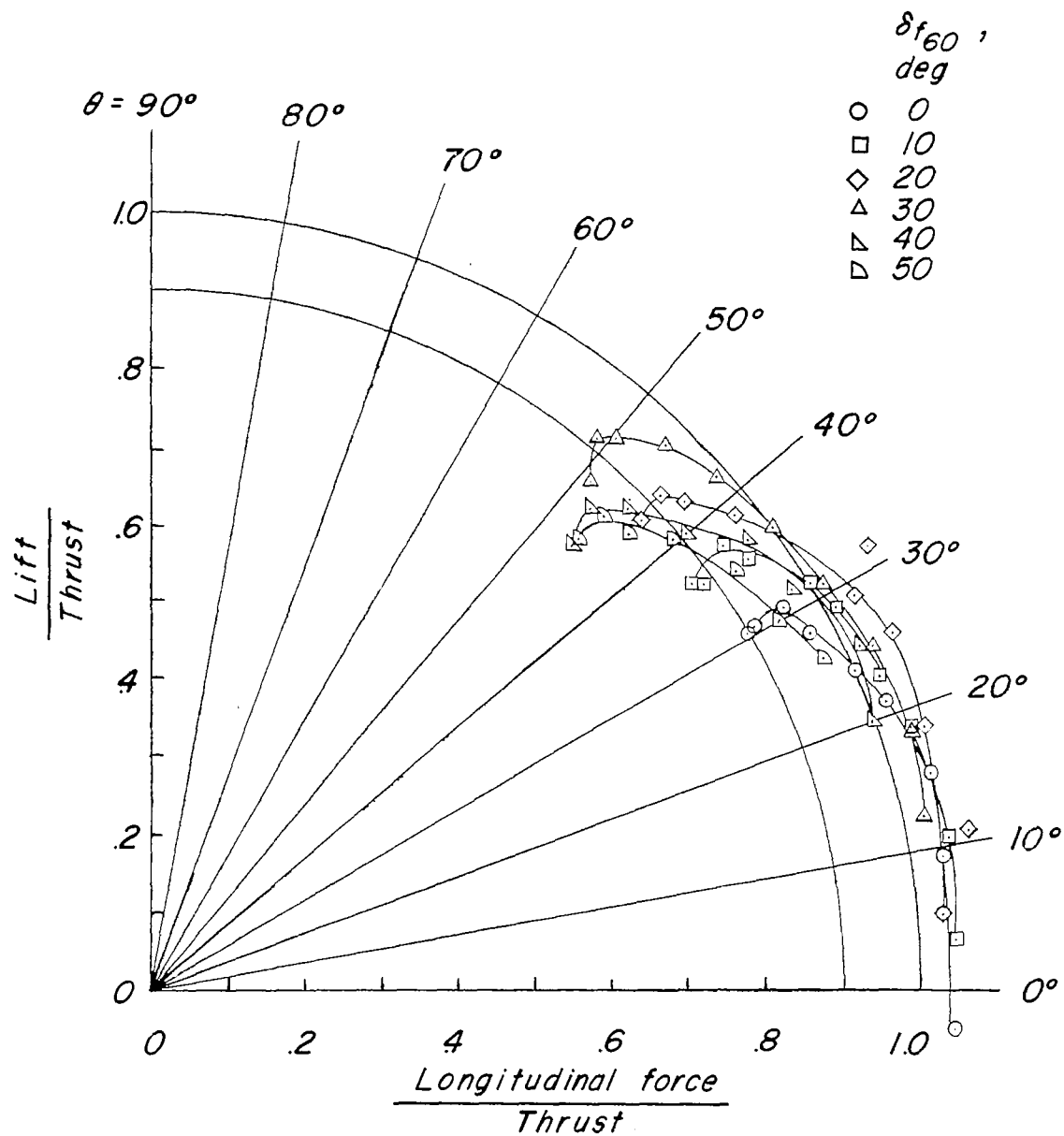


(b) Ratio of resultant force to thrust.



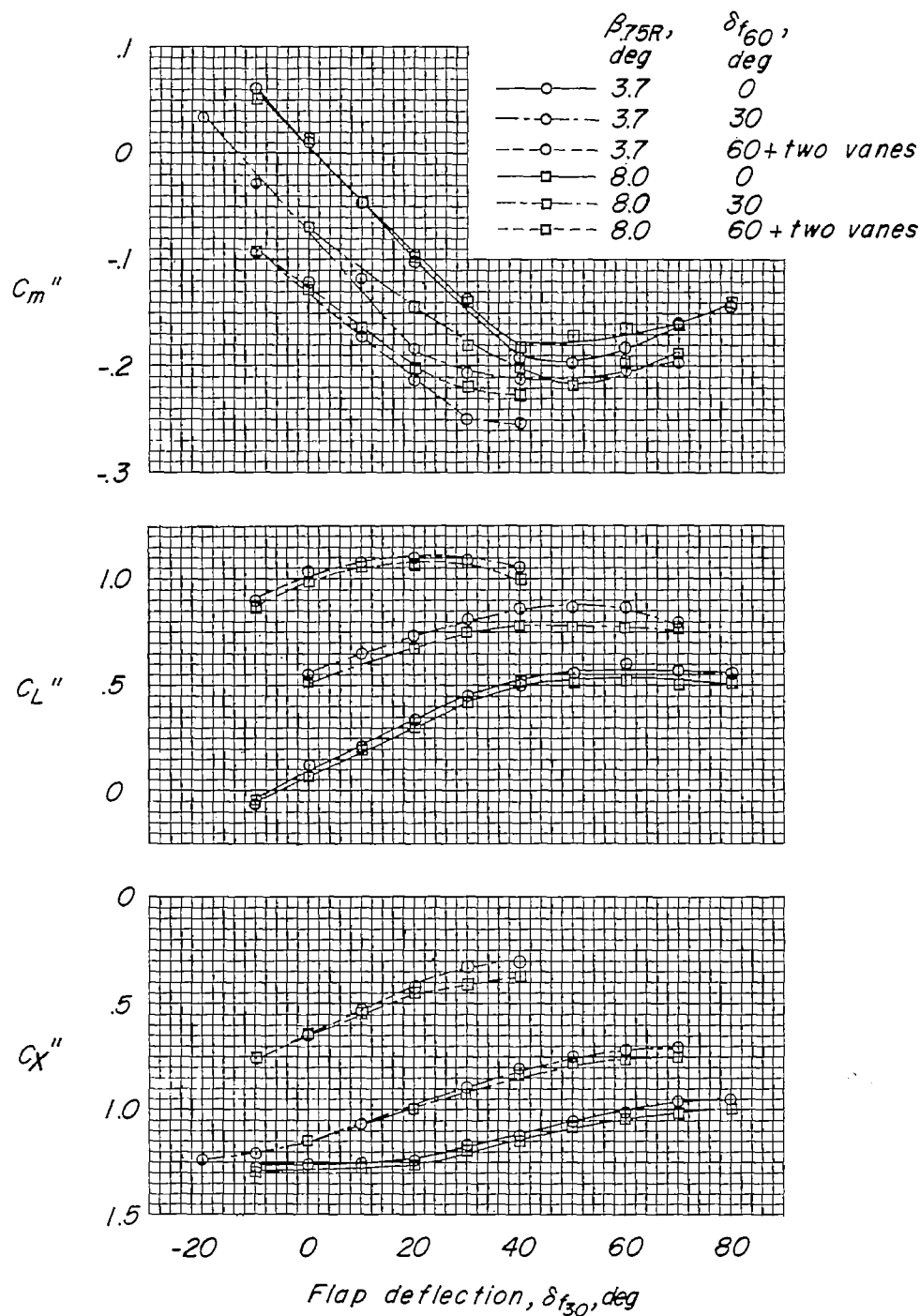
(c) Turning angle.

Figure 5.- Continued.



(d) Summary of turning effectiveness.

Figure 5.- Concluded.



(a) Pitching-moment, lift, and longitudinal-force coefficients.

Figure 6.- Effect of propeller blade angle and flap deflection on aerodynamic characteristics of wing in propeller slipstream at zero forward velocity. Two propellers; $T_c'' = 1.0$; $q'' = 8.0$ pounds per square foot; NACA 0015 airfoil.

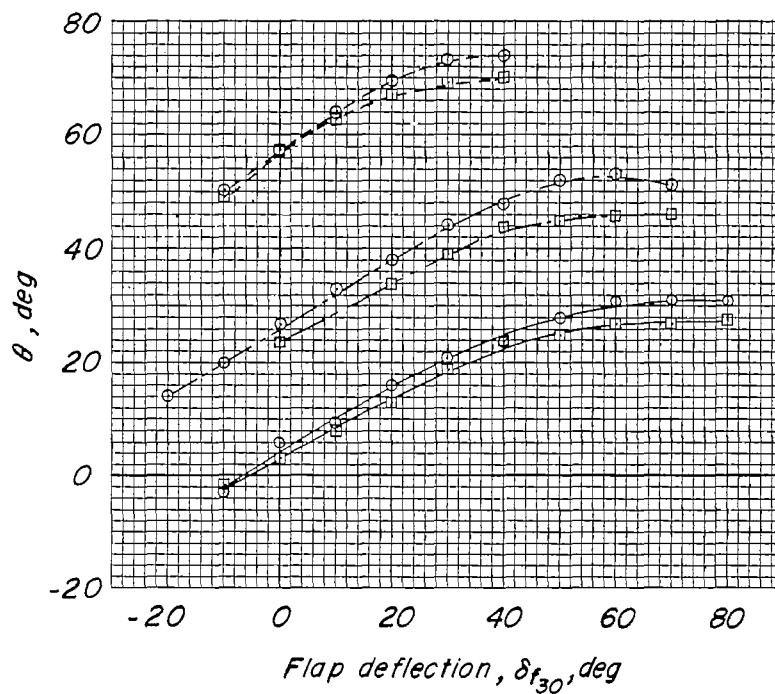
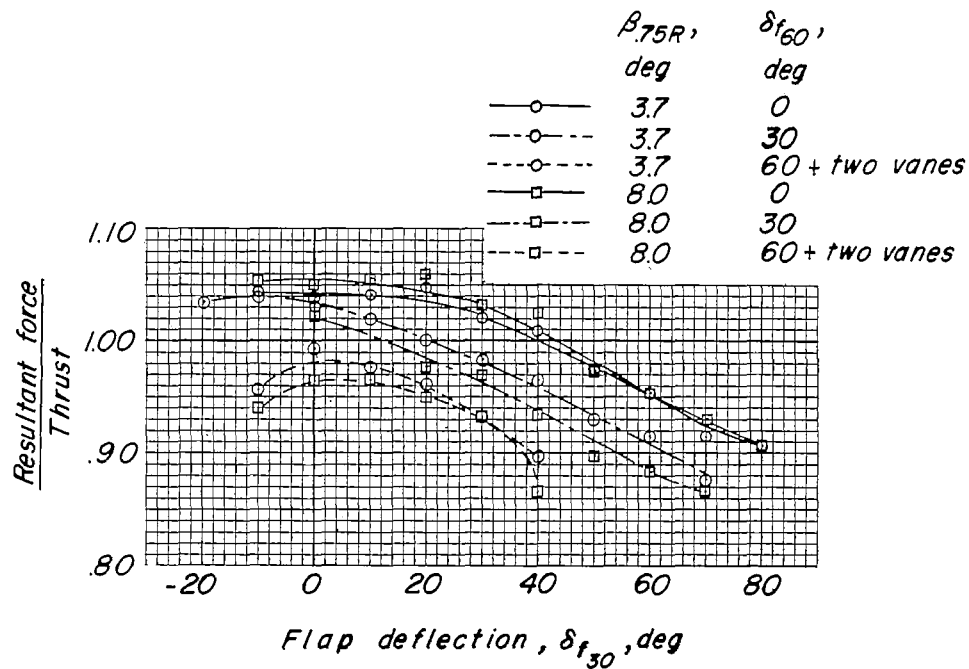
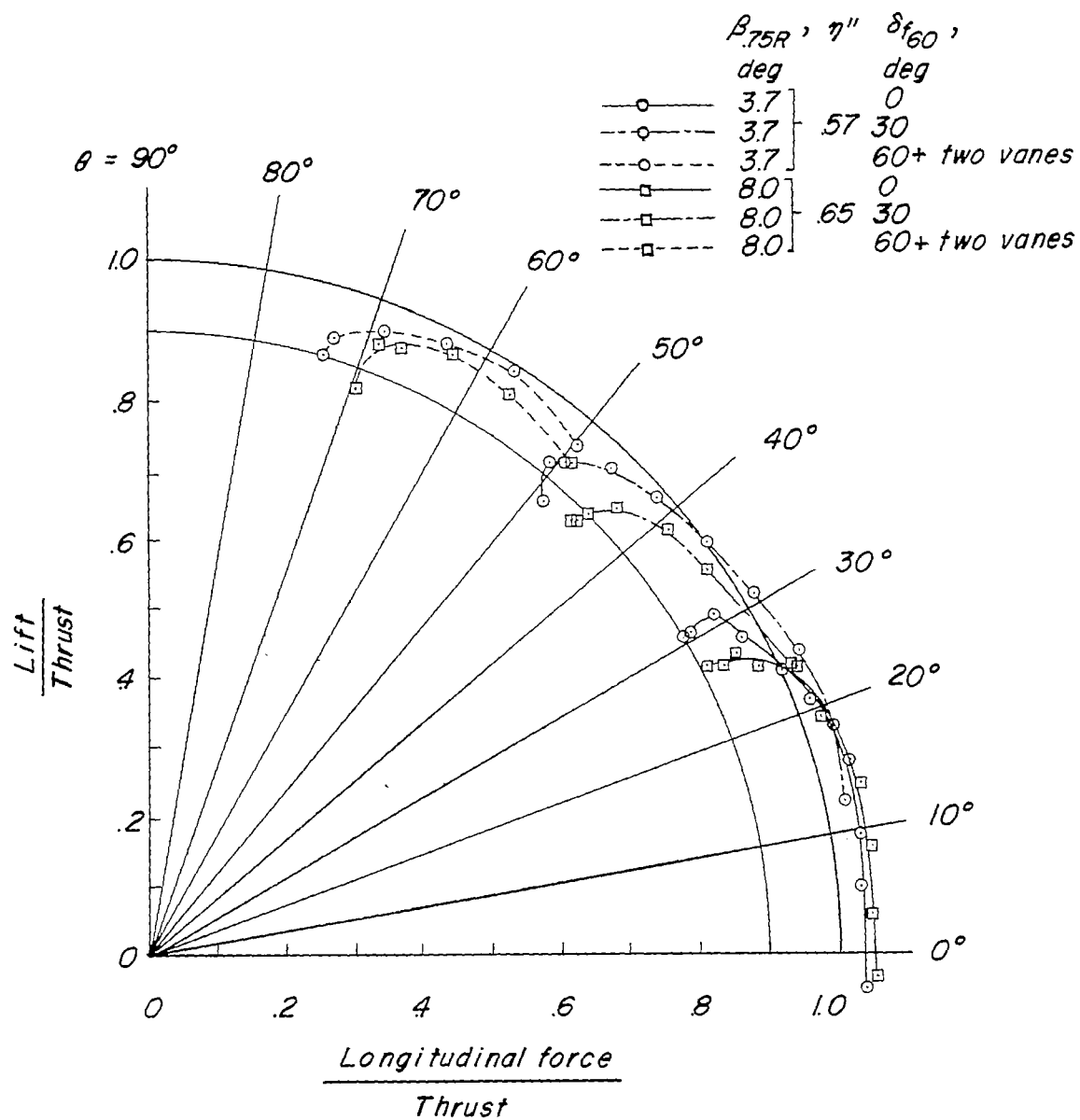
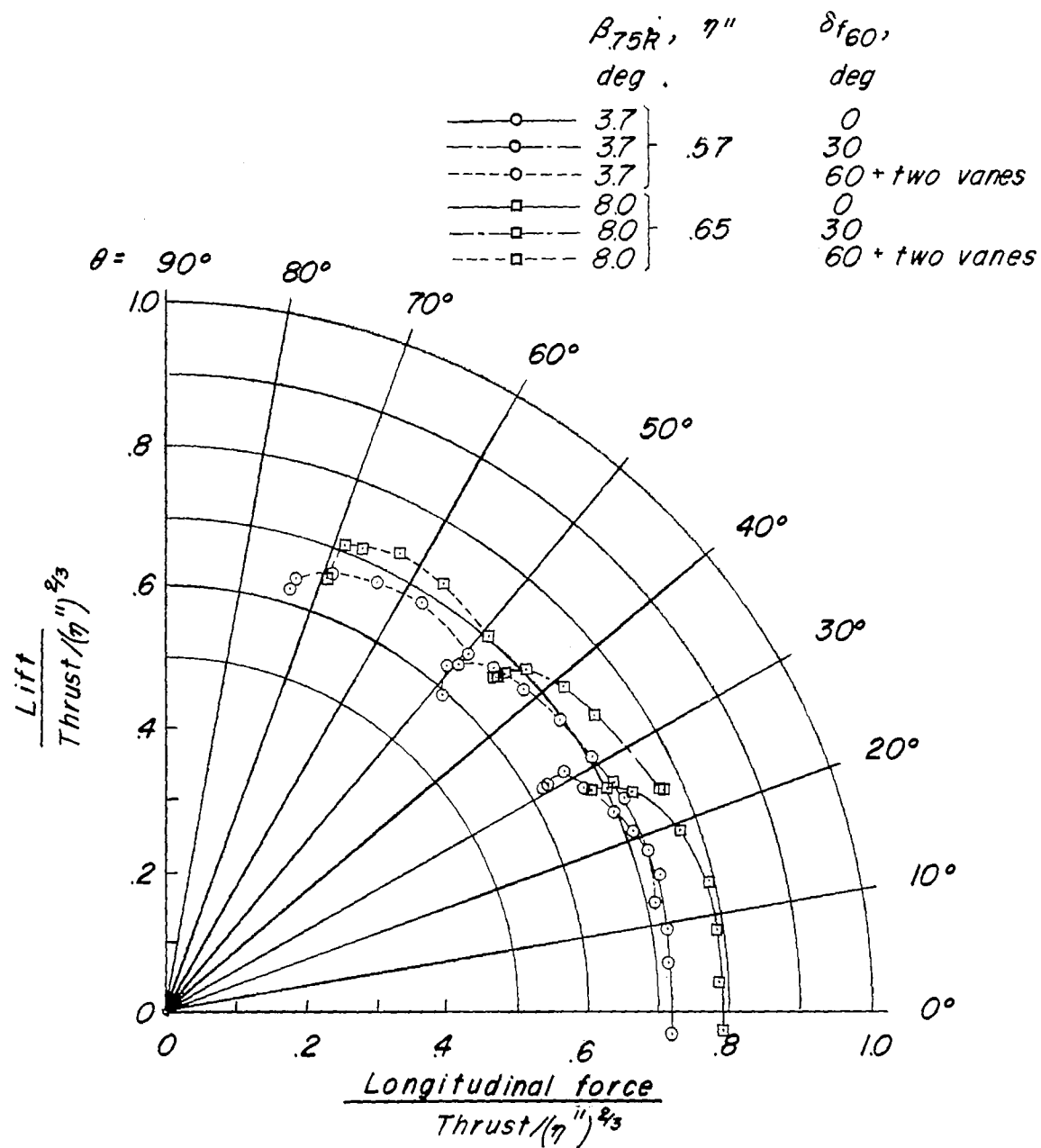


Figure 6.- Continued.



(d) Summary of turning effectiveness.

Figure 6.- Continued.



(e) Turning effectiveness based on power input.

Figure 6.- Concluded.

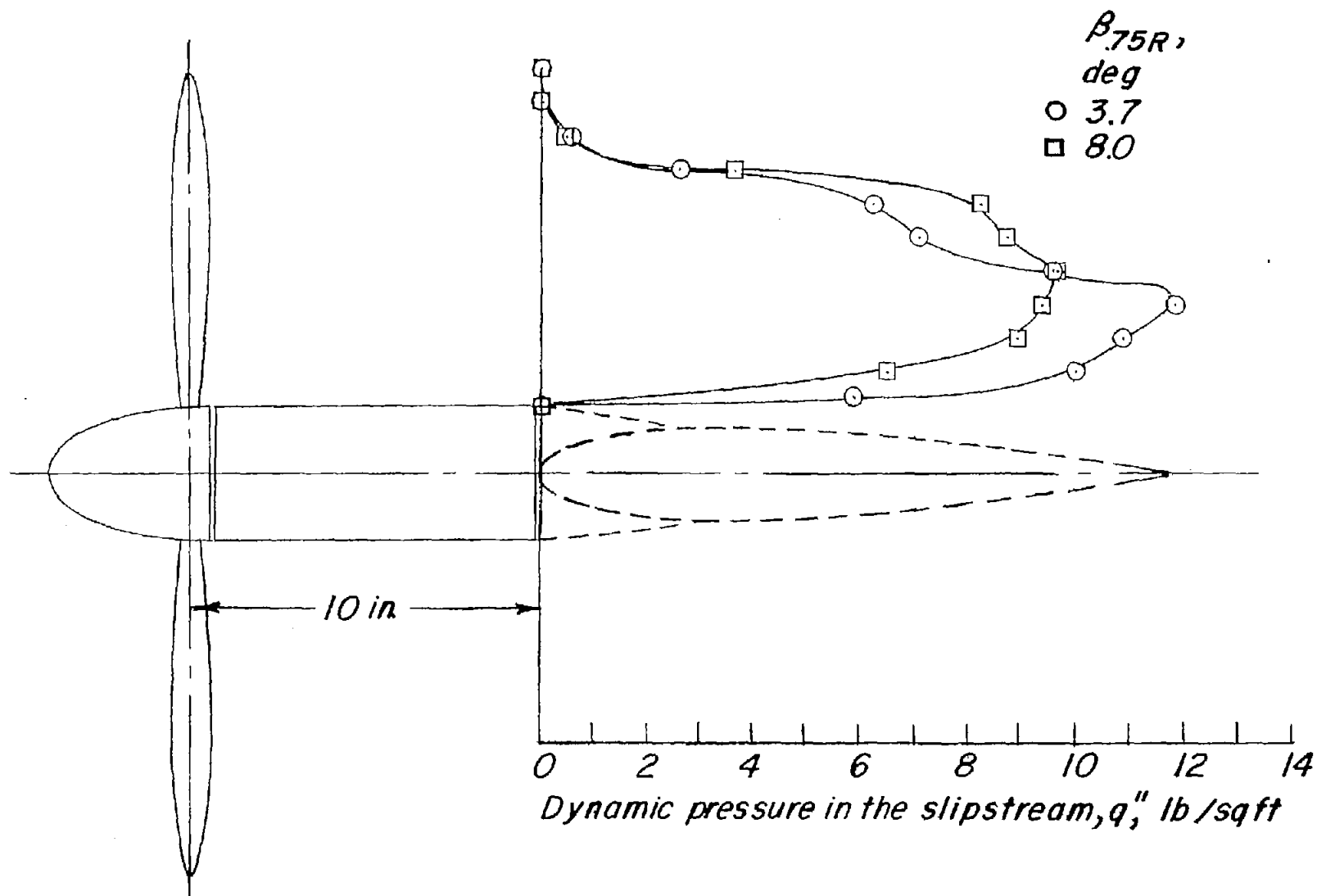
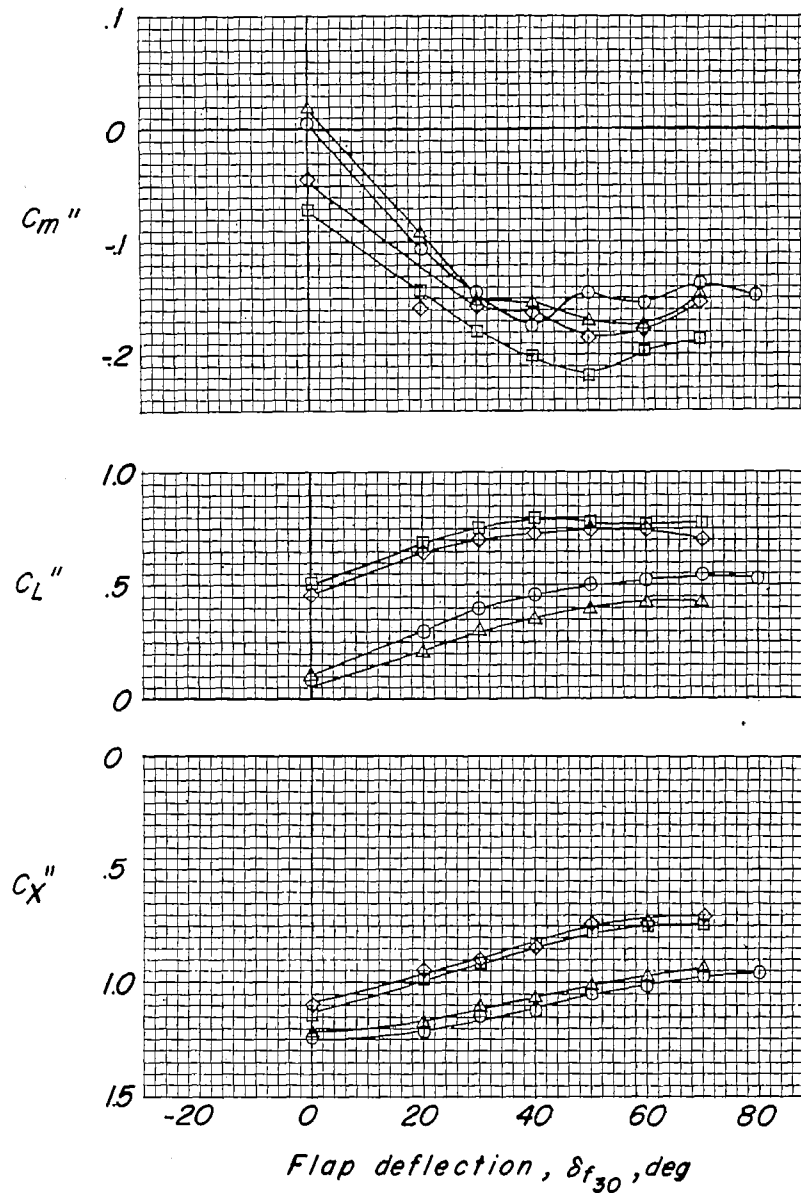


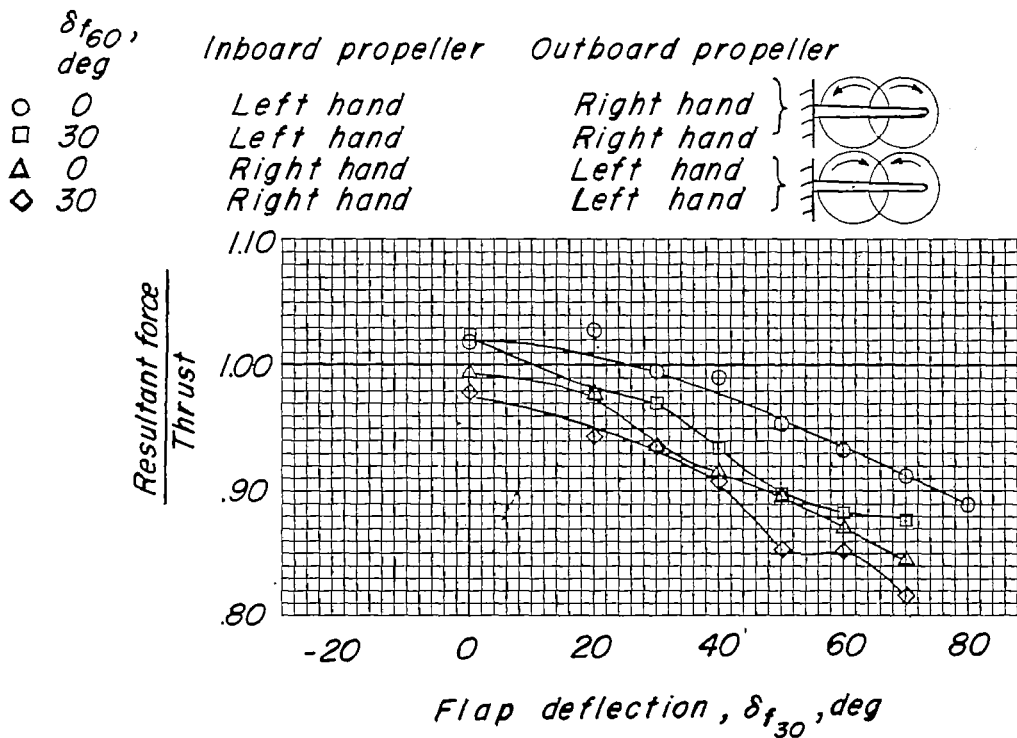
Figure 7.- Dynamic-pressure survey behind propeller. Wing removed; zero forward velocity; $T = 25$ pounds; $T_c'' = 1.0$.

δf_{60} , deg	Inboard propeller	Outboard propeller	
○ 0	Left hand	Right hand	
□ 30	Left hand	Right hand	
△ 0	Right hand	Left hand	
◇ 30	Right hand	Left hand	

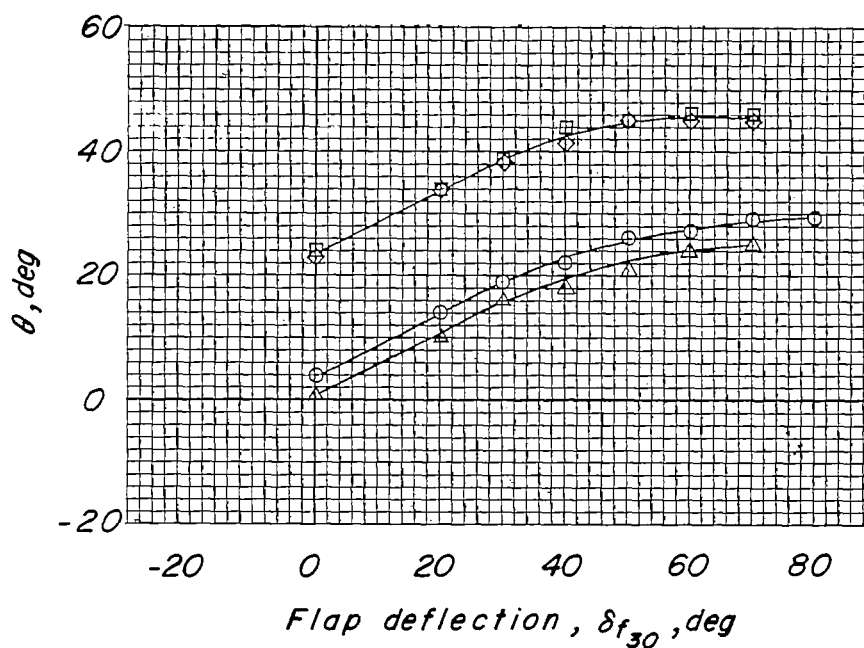


(a) Pitching-moment, lift, and longitudinal-force coefficients.

Figure 8.- Effect of direction of propeller rotation on aerodynamic characteristics of model representing right wing. $T_c'' = 1.0$; $\beta_{.75R} = 8.0^\circ$; $q'' = 8.0$ pounds per square foot; NACA 0015 airfoil.

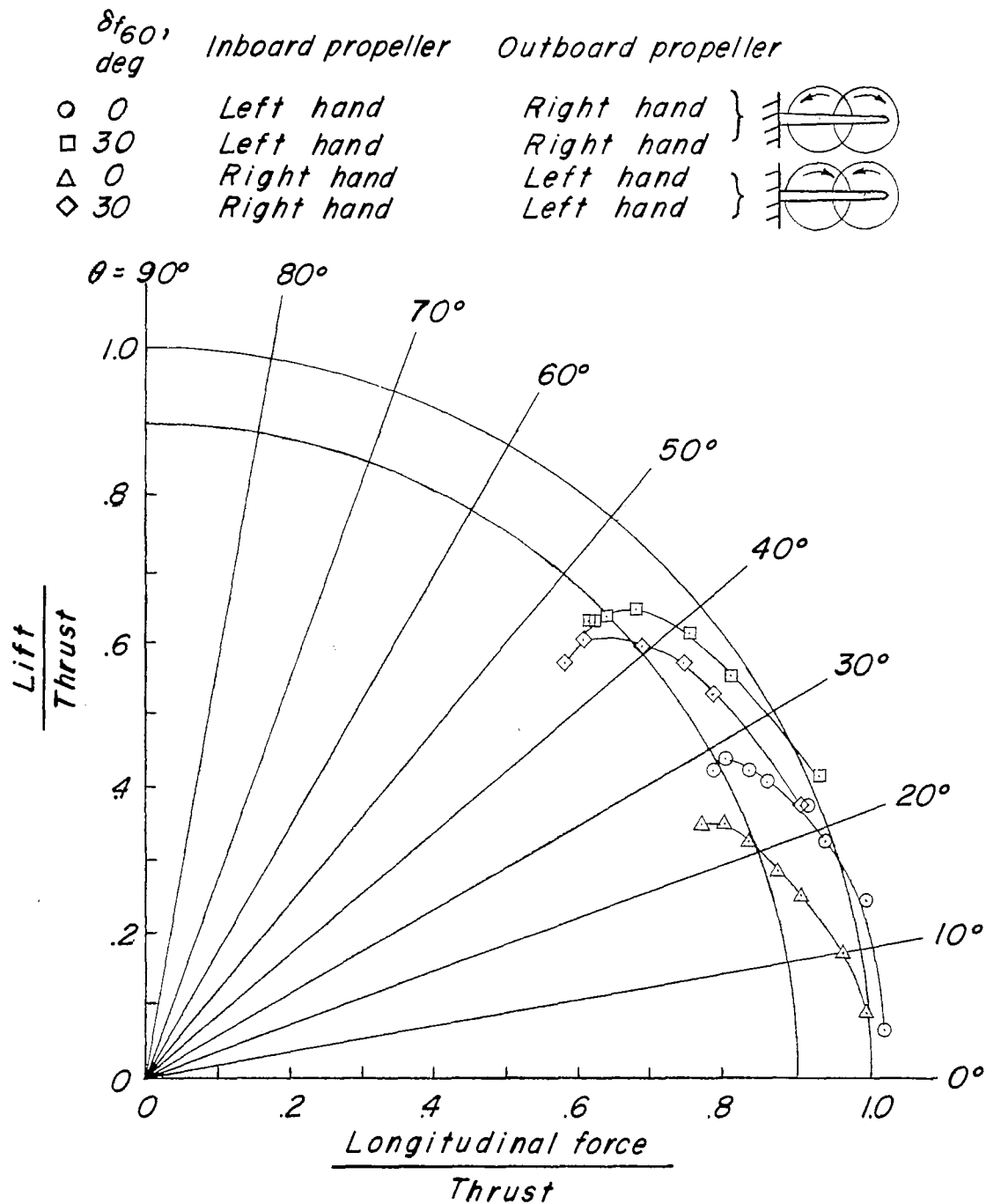


(b) Ratio of resultant force to thrust.



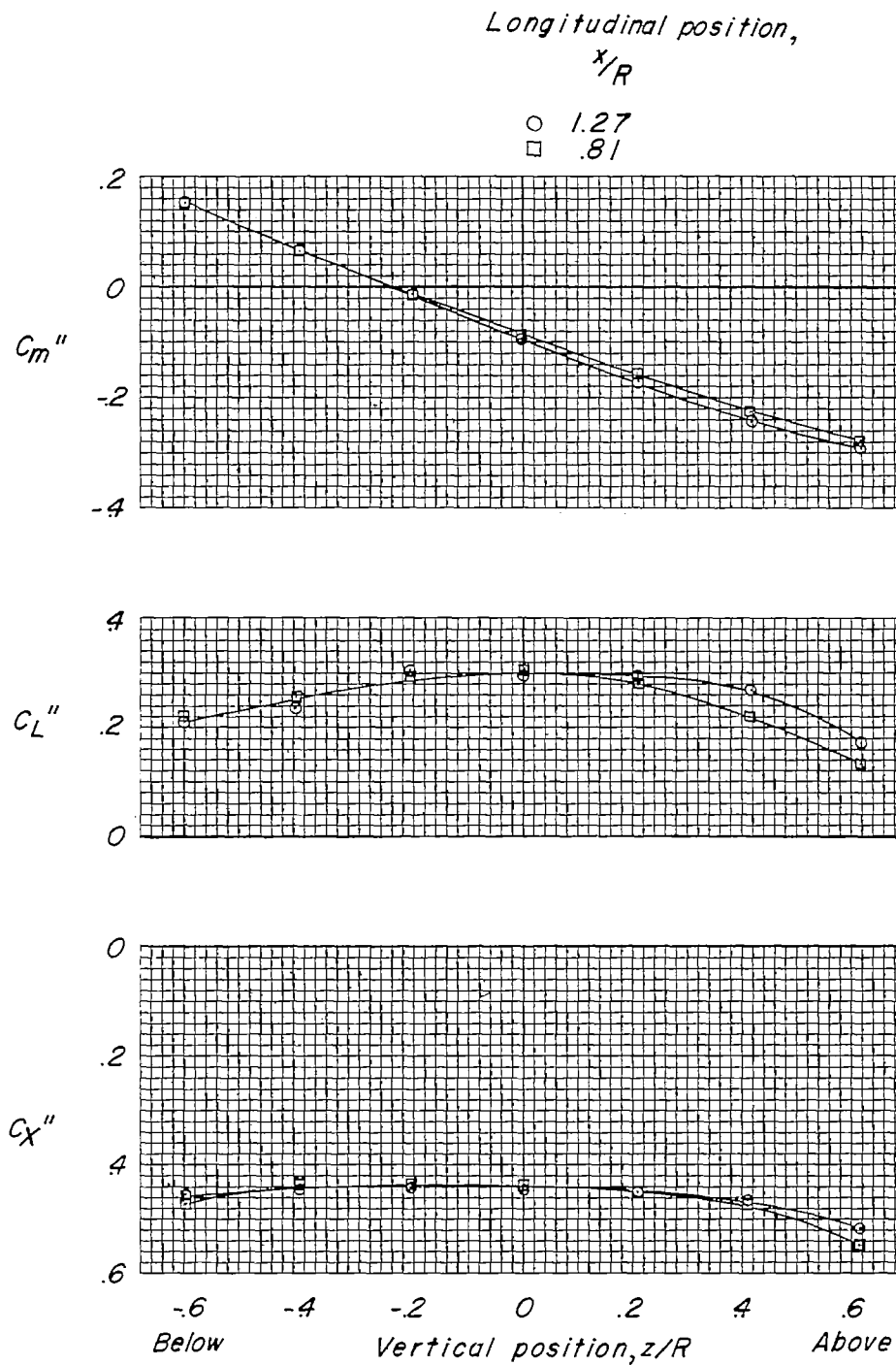
(c) Turning angle.

Figure 8.- Continued.



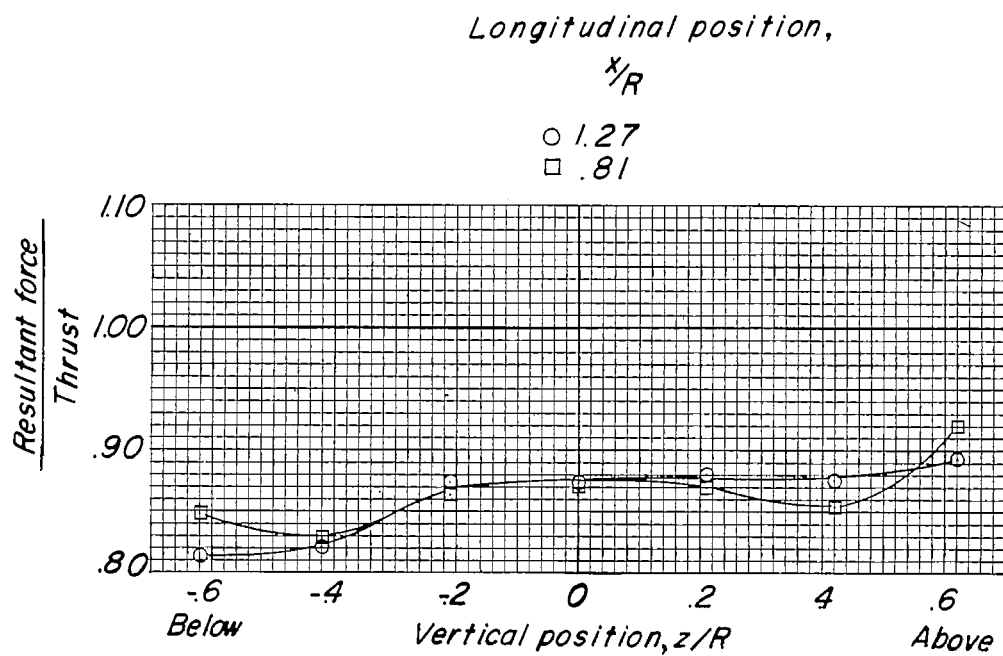
(d) Summary of turning effectiveness.

Figure 8.- Concluded.

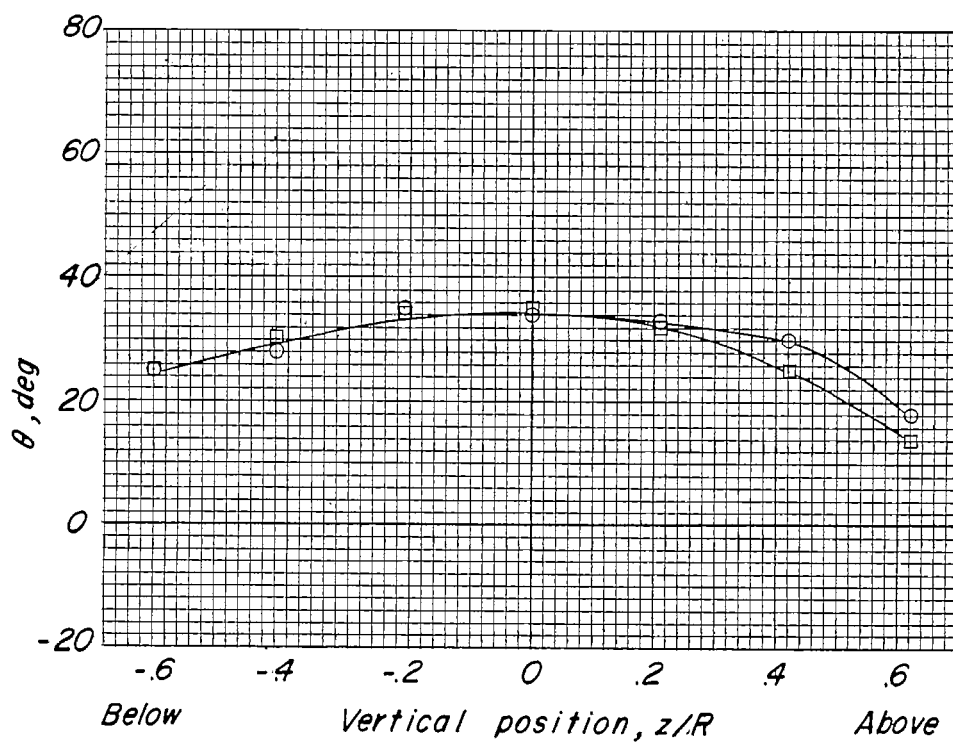


(a) Pitching-moment, lift, and longitudinal-force coefficients.

Figure 9.- Effect of propeller position relative to the wing. $\delta_{f_{30}} = 30^\circ$;
 $\delta_{f_{60}} = 30^\circ$; one propeller; $\beta_{.75R} = 8.0^\circ$; NACA 0015 airfoil.

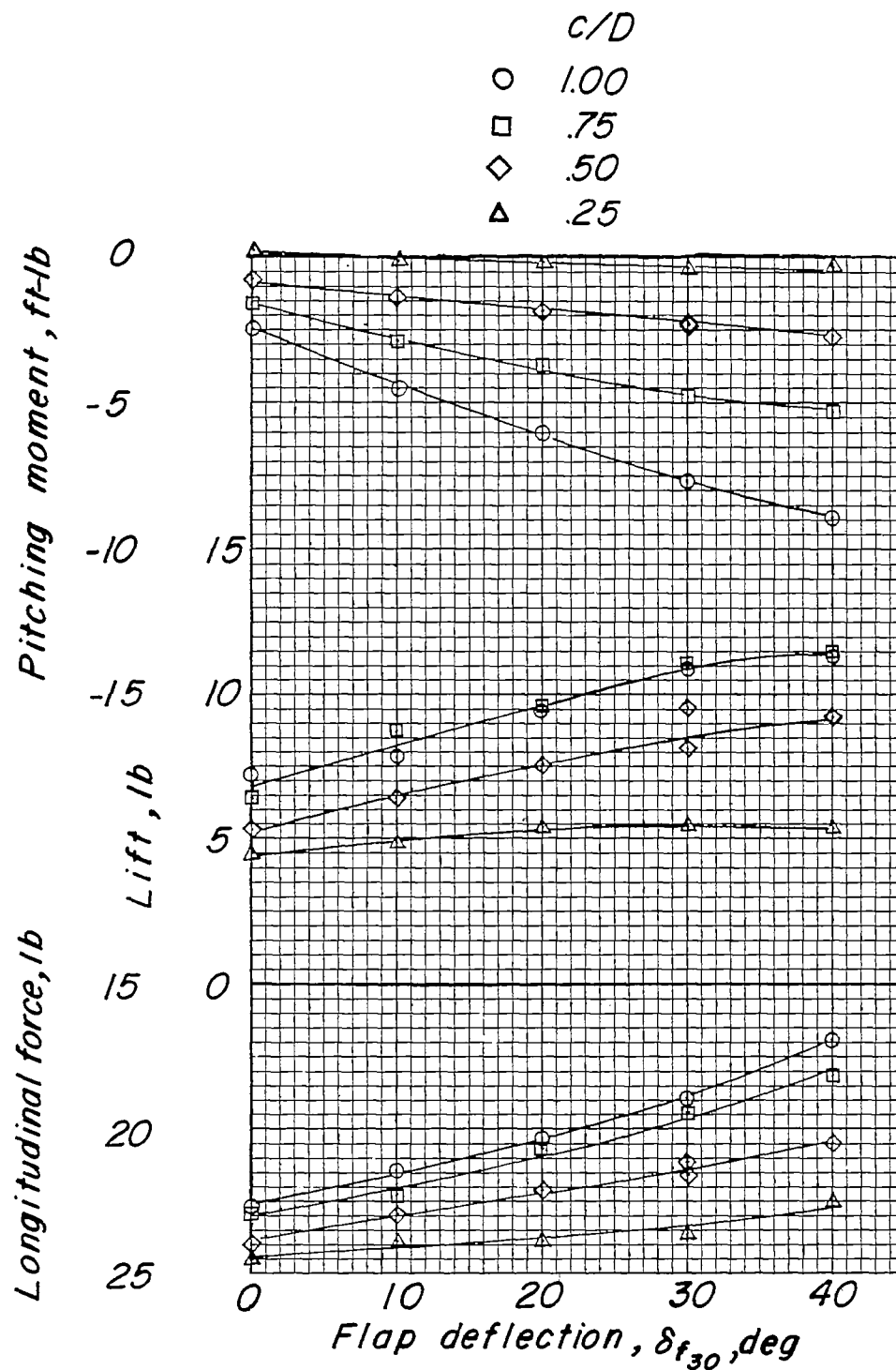


(b) Ratio of resultant force to thrust.



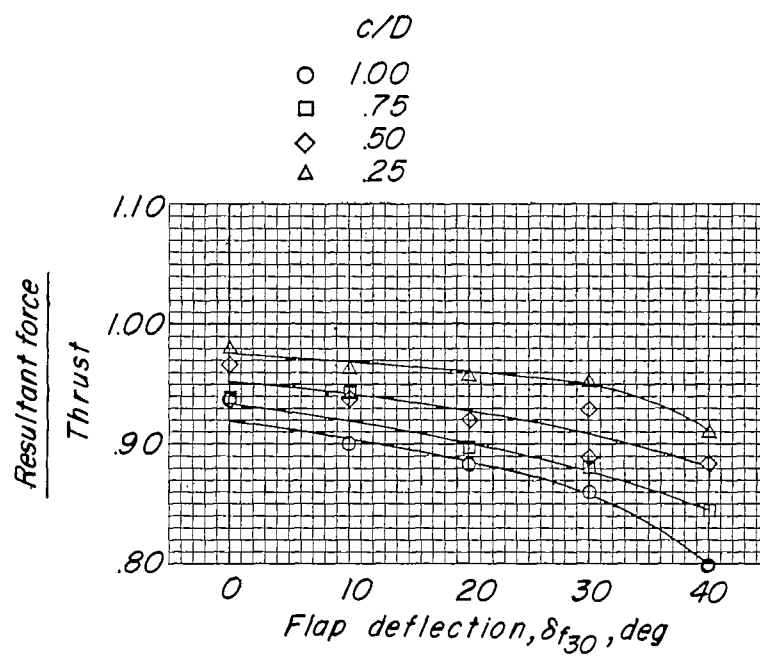
(c) Turning angle.

Figure 9.- Concluded.

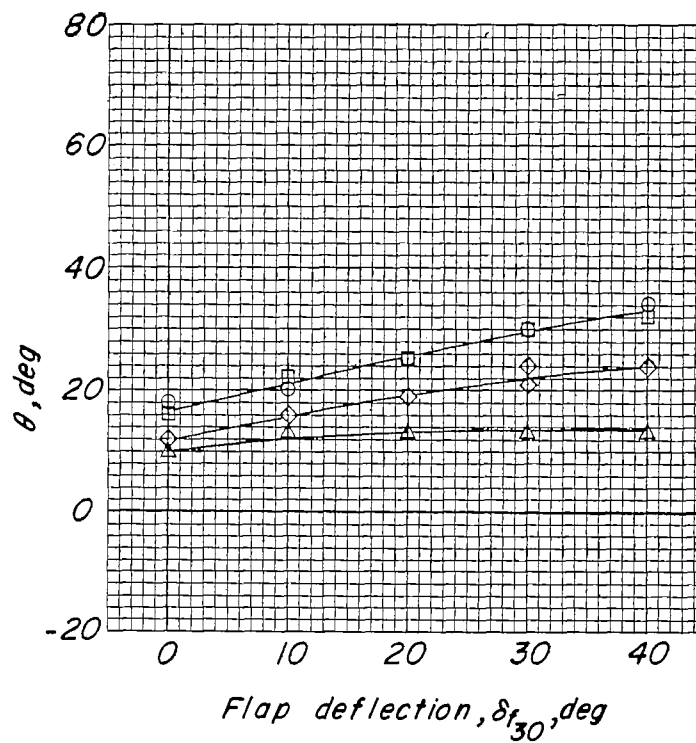


(a) Variation of forces and moments.

Figure 10.- Some effects of changing wing chord. One propeller; $\delta_{f60} = 30^\circ$;
 $T_c'' = 1.0$; $\beta_{.75R} = 8.0^\circ$; flat-plate airfoil.

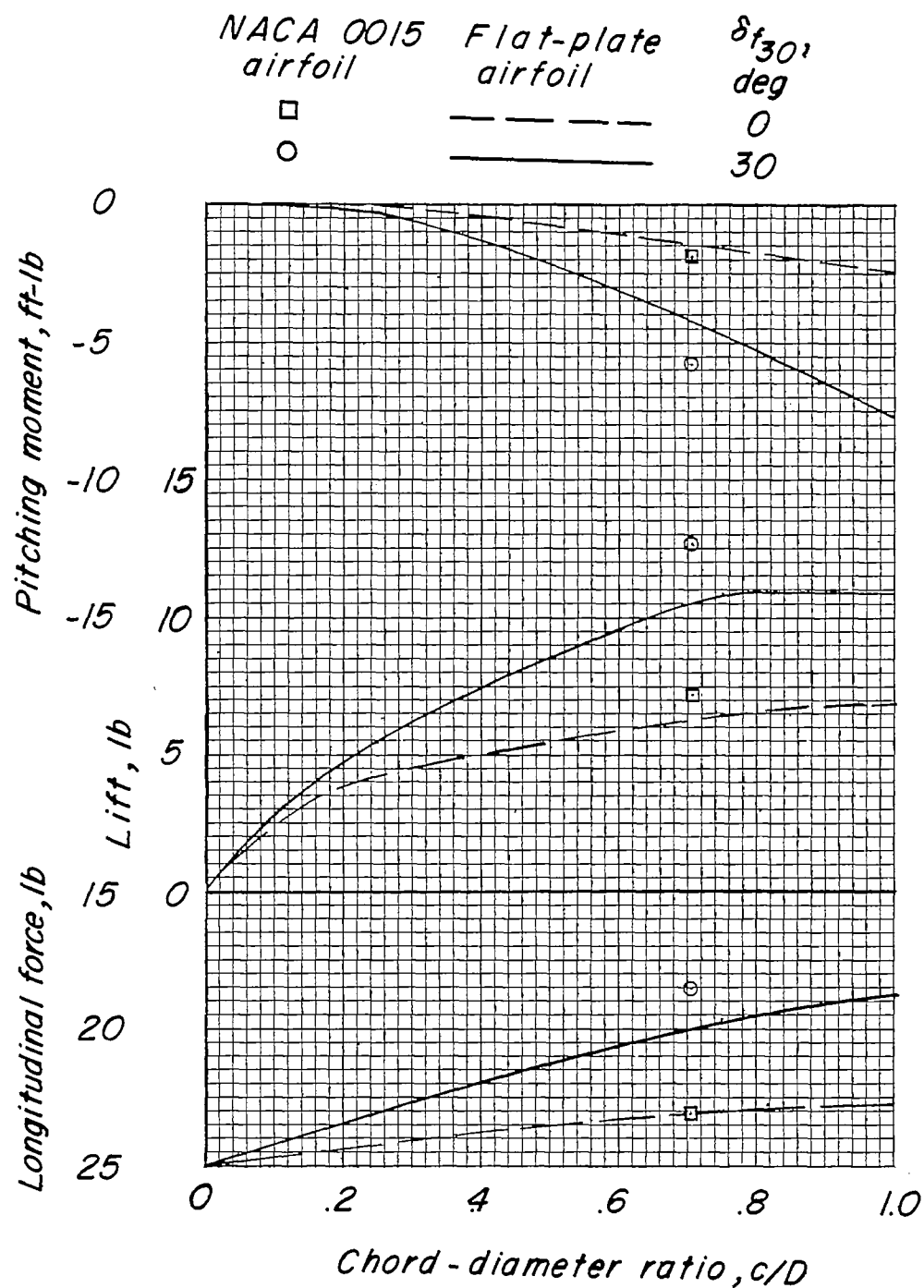


(b) Ratio of resultant force to thrust.



(c) Turning angle.

Figure 10.- Concluded.



(a) Variation of forces and moments.

Figure 11.- Effects of ratio of wing chord to propeller diameter on aerodynamic characteristics of a wing with flaps. One propeller; $\delta_{f60} = 30^\circ$;

$$T_c'' = 1.0; \beta_{.75R} = 8.0^\circ.$$

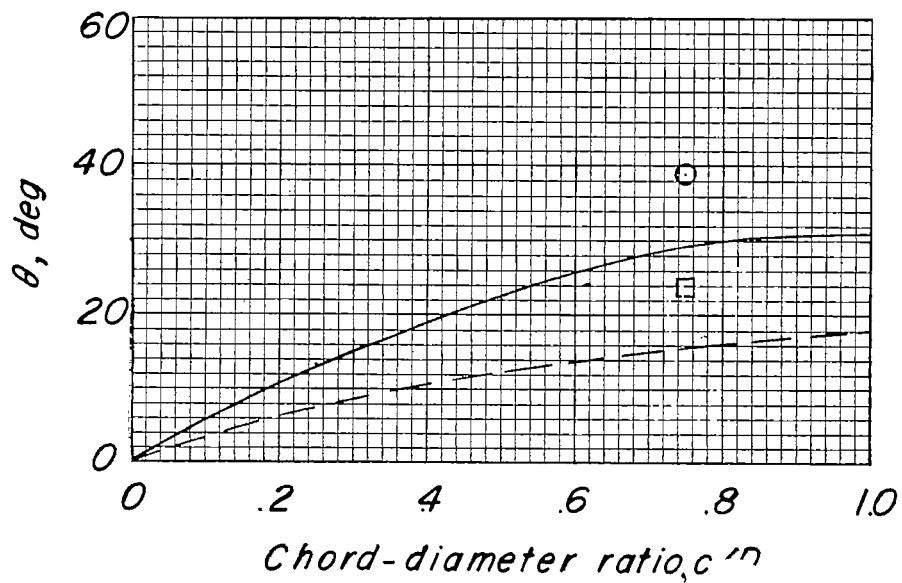
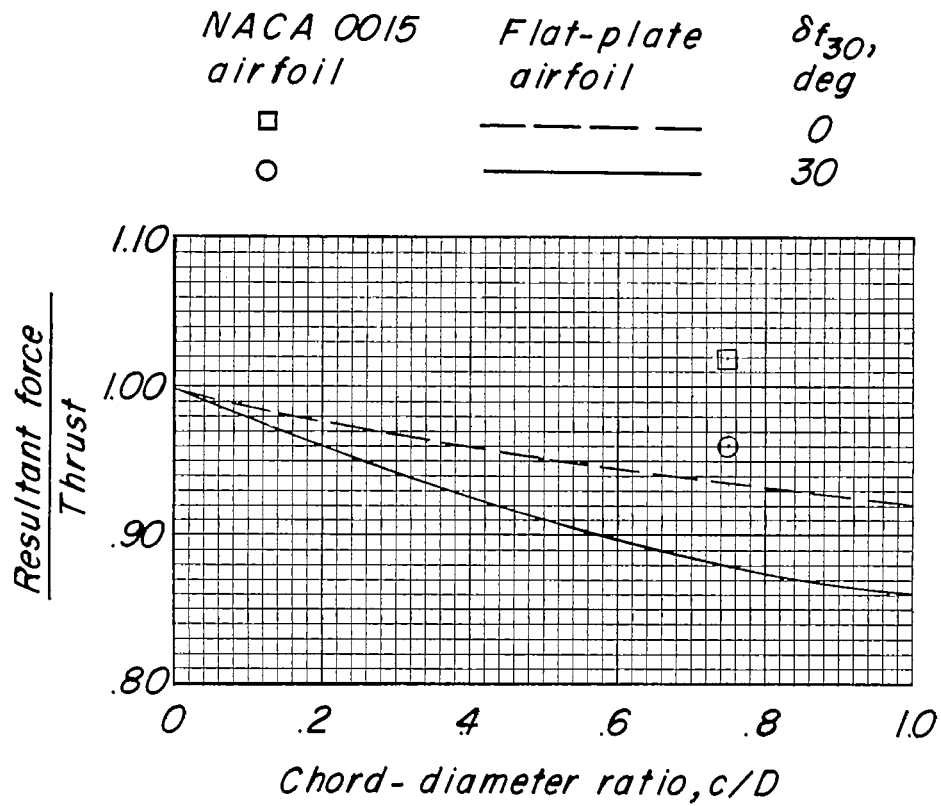


Figure 11.- Concluded.